AIAA Journal
Vol. 48, No. 12, December 2010

Point-Collocation Nonintrusive Polynomial Chaos Method for Stochastic Computational Fluid Dynamics

Serhat Hosder*
Missouri University of Science and Technology, Rolla, Missouri 65409
and
Robert W. Walters† and Michael Balch‡
Virginia Polytechnic Institute and State University, Blacksburg, Virginia 24061

DOI: 10.2514/1.39389

This paper describes a point-collocation nonintrusive polynomial chaos technique used for uncertainty propagation in computational fluid dynamics simulations. The application of point-collocation nonintrusive polynomial chaos to stochastic computational fluid dynamics is demonstrated with two examples: 1) a stochastic expansion-wave problem with an uncertain deflection angle (geometric uncertainty) and 2) a stochastic transonic-wing case with uncertain freestream Mach number and angle of attack. For each problem, input uncertainties are propagated with both the nonintrusive polynomial chaos method and Monte Carlo techniques to obtain the statistics of various output quantities. Confidence intervals for Monte Carlo statistics are calculated using the bootstrap method. For the expansion-wave problem, a fourth-degree polynomial chaos expansion, which requires five deterministic computational fluid dynamics evaluations, has been sufficient to predict the statistics within the confidence interval of 10,000 crude Monte Carlo simulations. In the transonic-wing case, for various output quantities of interest, it has been shown that a fifth-degree point-collocation nonintrusive polynomial chaos expansion obtained with Hammersley sampling was capable of estimating the statistics at an accuracy level of 1000 Latin hypercube Monte Carlo simulations with a significantly lower computational cost. Overall, the examples demonstrate that the point-collocation nonintrusive polynomial chaos has a promising potential as an effective and computationally efficient uncertainty propagation technique for stochastic computational fluid dynamics simulations.

Nomenclature

C_D	=	drag coefficient
C_L	=	lift coefficient
C_p	=	pressure coefficient
M_{ref}	=	reference (freestream) Mach number
N_t	=	number of terms in a total-order polynomial chaos expansion
n	=	number of random dimensions
n_p	=	oversampling ratio
p	=	order of polynomial chaos
$p(\boldsymbol{\xi})$	=	probability density function of $\boldsymbol{\xi}$
p_{ref}	=	reference (freestream) pressure
R	=	support region of random input variable
$\mathbf{x}$	=	deterministic independent variable vector
α	=	deterministic coefficient in the polynomial chaos expansion
α^*	=	generic uncertain flow variable
γ	=	ratio of specific heats
θ	=	flow deflection angle
μ	=	mean value
$\boldsymbol{\xi}$	=	n-dimensional standard input random variable vector
σ^2	=	variance
Ψ	=	random basis function

Received 26 June 2008; revision received 11 March 2010; accepted for publication 10 August 2010.

*Assistant Professor of Aerospace Engineering, Mechanical and Aerospace Engineering, 290B Toomey Hall. Senior Member AIAA.

†Vice President for Research, 301 Burruss Hall. Associate Fellow AIAA.

‡Graduate Student, Aerospace and Ocean Engineering, 215 Randolph Hall. Student Member AIAA.

I. Introduction

A DETERMINISTIC computational fluid dynamics (CFD) simulation gives a single solution for a certain set of input parameters (the geometry, freestream flow conditions, angle of attack, etc.). In real life, these parameters are mostly uncertain and the variability associated with them can have substantial impact on the final result. Stochastic CFD simulations are needed to assess the uncertainty in the solution and to achieve a certain level of robustness or reliability in the final aerodynamic design. Development of credible stochastic aerodynamic simulation tools require effective and computationally efficient methods to model and propagate the input uncertainties, and sufficient testing on various fluid dynamics problems. Here, we address this requirement by introducing the point-collocation nonintrusive polynomial chaos (NIPC) method developed for the uncertainty propagation in CFD simulations and apply the method to selected stochastic CFD problems.

Several methods have been used to model and propagate uncertainty in stochastic computational simulations. Interval analysis, propagation of uncertainty using sensitivity derivatives, Monte Carlo simulations, moment methods and polynomial chaos are among the main approaches implemented in CFD simulations. Detailed description and analysis of each method for selected fluid dynamics problems can be found in Walters and Huyse [1]. In this paper we focus on uncertainty propagation with the polynomial chaos (PC) method, which is based on the spectral representation of the uncertainty. Several researchers have studied and implemented the polynomial chaos (PC) approach for a wide range of problems. Ghanem and Spanos [2,3] and Ghanem [4,5] applied the PC method to several problems of interest to the structures community. Mathelin et al. [6] studied uncertainty propagation for a turbulent, compressible nozzle flow by this technique. Xiu and Karniadakis [7] analyzed the flow past a circular cylinder and incompressible channel flow by the PC method and extended the method beyond the original formulation of Wiener [8] to include a variety of basis functions. In 2003, Walters [9] applied the PC method to a two-dimensional steady-state heat conduction problem for representing geometric uncertainty. Following this effort, an implicit compact PC formulation was implemented for the stochastic Euler equations (Perez and Walters [10]). A comprehensive review of uncertainty quantification and polynomial chaos techniques in CFD is given in a recent paper by Najm [11].

The polynomial chaos method for the propagation of uncertainty in computational simulations involves the substitution of uncertain variables and parameters in the governing equations with the polynomial expansions. In general, an intrusive approach will calculate the unknown polynomial coefficients by projecting the resulting equations onto basis functions (orthogonal polynomials) for different modes. As its name suggests, the intrusive approach requires the modification of the deterministic code and this may be difficult, expensive, and time-consuming for many complex computational problems such as the full Navier–Stokes simulation of 3-D viscous turbulent flows around aerospace vehicles, chemically reacting flows, numerical modeling of planetary atmospheres, or multisystem level simulations which include the interaction of many different codes from different disciplines. To overcome such inconveniences associated with the intrusive approach, nonintrusive polynomial chaos formulations have been developed for uncertainty propagation. Most of the NIPC approaches in the literature are based on sampling (Debusschere et al. [12], Reagan et al. [13], and Isukapalli [14]) or quadrature-based methods (Debusschere et al. [12] and Mathelin et al. [15]) to determine the projected polynomial coefficients. A nonintrusive probabilistic collocation approach for efficient propagation of arbitrarily distributed parametric uncertainties was introduced by Loeven et al. [16].

In the following section, the basics of polynomial chaos theory are described. Next, the point-collocation NIPC method is introduced. In Sec. IV, the application of point-collocation NIPC to stochastic CFD simulations is demonstrated with two examples: 1) stochastic expansion-wave problem with geometric uncertainty and 2) stochastic transonic-wing case with uncertain freestream Mach number and angle of attack. For each problem, input uncertainties are propagated both with the NIPC method and Monte Carlo techniques to obtain the statistics of various output quantities and a detailed analysis of results are presented. The conclusions are given in Sec. V.

II. Basics of Polynomial Chaos Theory

The polynomial chaos is a stochastic method based on the spectral representation of the uncertainty. An important aspect of spectral representation of uncertainty is that one may decompose a random function (or variable) into separable deterministic and stochastic components. For example, for any random variable (i.e., α^*) such as velocity, density, or pressure in a stochastic fluid dynamics problem, we can write

$$\alpha^*(\mathbf{x},\boldsymbol{\xi}) \approx \sum_{j=0}^{P} \alpha_j(\mathbf{x})\Psi_j(\boldsymbol{\xi}) \tag{1}$$

where $\alpha_j(\mathbf{x})$ is the deterministic component and $\Psi_j(\boldsymbol{\xi})$ is the random basis function corresponding to the jth mode. Here, we assume α^* to be a function of deterministic independent variable vector $\mathbf{x}$ and the n-dimensional standard random variable vector $\boldsymbol{\xi} = (\xi_1,\ldots,\xi_n)$. In theory, the polynomial chaos expansion given by Eq. (1) should include infinite number of terms, however, in practice a discrete sum is taken over a number of output modes (or total number of terms, N_t) for a total-order expansion given by

$$N_t = P + 1 = \frac{(n+p)!}{n!p!} \tag{2}$$

which is a function of the order of polynomial chaos p and the number of random dimensions n. The basis functions used in the stochastic expansion given in Eq. (1) are polynomials that are orthogonal with respect to a weight function over the support region of the input random variable vector. The basis function takes the form of a multidimensional Hermite polynomial to span the n-dimensional random space when the input uncertainty is Gaussian (normal), which was originally used by Wiener [8] and Weiner and Wintner [17]. To extend the application of the polynomial chaos theory to the propagation of continuous non-normal-input uncertainty distributions, Xiu and Karniadakis [7] used a set of polynomials known as the Askey scheme to obtain the Wiener– Askey generalized polynomial chaos. The Legendre and Laguerre polynomials are optimal basis functions for uniform and exponential input uncertainty distributions, respectively, whereas the Hermite polynomials are optimal for the normal distributions in terms of the convergence of the statistics [18]. The optimality of the selection of these basis functions derives from the inner product weighting functions that correspond to the probability density functions of the continuous input uncertainty distributions represented in standard form.

The multivariate basis functions can be obtained from the product of univariate orthogonal polynomials. As an example, multivariate Hermite polynomials can be calculated by

$$H_n(\xi_{i1},\ldots,\xi_{in}) = H_n(\boldsymbol{\xi}) = e^{\frac{1}{2}\boldsymbol{\xi}^T\boldsymbol{\xi}}(-1)^n \frac{\partial^n}{\partial\xi_{i1},\ldots,\xi_{in}} e^{-\frac{1}{2}\boldsymbol{\xi}^T\boldsymbol{\xi}} \tag{3}$$

If the probability distribution of each random variable is different, then the optimal multivariate basis functions can be obtained by employing the optimal univariate polynomial at each random dimension. This approach requires that the input uncertainties are independent standard random variables, which also allows the calculation of the multivariate weight functions by the product of univariate weight functions associated with the probability distribution at each random dimension. The generalized polynomial chaos approach can be applied to the propagation of any independent random variable included in the Askey scheme. If the input uncertainties are correlated or have arbitrary distributions that are not covered in the Askey scheme, alternative approaches can be employed. One approach is to use nonlinear variable transformations [19] so that the Askey basis can be applied in the transformed space. Despite its effectiveness, this method can reduce the convergence rate of the statistics. Another approach is to apply Gram–Schmidt orthogonalization for numerically generating the orthogonal polynomials along with their Gauss points and weights, which are optimal for given input uncertainties with arbitrary probability density functions [20].

The objective of the stochastic methods based on polynomial chaos is to determine the coefficient of each term ($\alpha_j(\mathbf{x})$, $j = 0,\ldots,P$) in the polynomial expansion given by Eq. (1). The statistics of the distribution for a flow variable at a spatial location can then be calculated using the coefficients and the orthogonality of the basis functions. For example, the mean of the random solution is given by

$$\mu_{\alpha^*} = \bar{\alpha}^*(\mathbf{x}) = \int_R \alpha^*(\mathbf{x},\boldsymbol{\xi})p(\boldsymbol{\xi})\,\mathrm{d}\boldsymbol{\xi} = \alpha_0(\mathbf{x}) \tag{4}$$

which indicates that the zeroth mode of the expansion corresponds to the expected value or the mean of $\alpha^*(\mathbf{x},\boldsymbol{\xi})$. Similarly, the variance of the distribution can be obtained as

$$\begin{aligned}\sigma^2_{\mathrm{a}^*} &= \mathrm{Var}[\alpha^*(\mathbf{x},\boldsymbol{\xi})] = \int_R (\alpha^*(\mathbf{x},\boldsymbol{\xi}) - \bar{\alpha}^*_0(\mathbf{x}))^2 p(\boldsymbol{\xi})\,\mathrm{d}\boldsymbol{\xi}\\ &= \sum_{j=1}^{P}[\alpha_j^2(\mathbf{x})\langle\Psi_j^2(\boldsymbol{\xi})\rangle]\end{aligned} \tag{5}$$

In the above two equations, we have used the fact that $\langle\Psi_j(\boldsymbol{\xi})\rangle = 0$ for $j > 0$ and $\langle\Psi_i(\boldsymbol{\xi})\Psi_j(\boldsymbol{\xi})\rangle = \langle\Psi_j^2(\boldsymbol{\xi})\rangle\delta_{ij}$. Here, the inner product of $\Psi_i(\boldsymbol{\xi})$ and $\Psi_j(\boldsymbol{\xi})$ in the support region R is given as

$$\langle\Psi_i(\boldsymbol{\xi})\Psi_j(\boldsymbol{\xi})\rangle = \int_R \Psi_i(\boldsymbol{\xi})\Psi_j(\boldsymbol{\xi})p(\boldsymbol{\xi})\,\mathrm{d}\boldsymbol{\xi} \tag{6}$$

where $p(\boldsymbol{\xi})$ is the weight function. Note that although we have written Eq. (1) for an uncertain flow quantity at a spatial location in the flowfield, the same equation can be used to represent the integrated flow quantities such as the lift and drag coefficients in a stochastic aerodynamics problem, and the associated statistics can be calculated using Eqs. (4) and (5).

To model the uncertainty propagation in computational simulations via polynomial chaos with an intrusive approach, all dependent variables and random parameters in the governing equations are replaced with their polynomial chaos expansions. Taking the inner product of the equations, (or projecting each equation onto jth basis) yield N_t times the number of deterministic equations which can be solved by the same numerical methods applied to the original deterministic system. For a detailed description of the application of the intrusive polynomial chaos to governing equations of the fluid dynamics (see [1,6,7,10,11]). To implement an intrusive polynomial chaos to an existing simulation code, almost the whole program has to be rewritten. Although straightforward in theory, an intrusive formulation for complex problems such as the full Navier–Stokes simulation of 3-D, viscous, turbulent flows around realistic aerospace vehicles, chemically reacting flows, or multisystem level simulations which include the interaction of many different codes from different disciplines can be difficult to implement. To overcome such inconveniences associated with the intrusive approach, nonintrusive polynomial chaos formulations are considered for uncertainty propagation.

The main objective of the nonintrusive polynomial chaos methods (NIPC) is to obtain the polynomial coefficients without making any modifications to the deterministic code. This approach treats the deterministic CFD model as a black box and approximates the polynomial coefficients with formulas based on deterministic code evaluations. The strategy for the selection of points in random space for deterministic code evaluations and the number of these points depend on the nonintrusive technique used. The ideal nonintrusive method would predict the polynomial coefficients with minimum number of deterministic evaluations at the desired accuracy level for a given stochastic problem. In addition to the method presented in this paper, the other approaches for nonintrusive polynomial chaos are based on spectral projection (sampling and quadrature-based methods). A brief description of these methods is given in the Appendix.

III. Point-Collocation Nonintrusive Polynomial Chaos

The collocation based NIPC starts with replacing the uncertain variables of interest with their polynomial expansions given by Eq. (1). Then, $P+1$ (N_t) vectors ($\boldsymbol{\xi}_i = \{\xi_1, \xi_2, \ldots, \xi_n\}_i$, $i = 0, 1, 2, \ldots, P$) are chosen in random space for a given PC expansion with $P+1$ modes and the deterministic CFD code is evaluated at these points. With the left-hand side of Eq. (1) known from the solutions of deterministic evaluations at the chosen random points, a linear system of equations can be obtained:

$$\begin{bmatrix} \Psi_0(\boldsymbol{\xi}_0) & \Psi_1(\boldsymbol{\xi}_0) & \cdots & \Psi_P(\boldsymbol{\xi}_0) \\ \Psi_0(\boldsymbol{\xi}_1) & \Psi_1(\boldsymbol{\xi}_1) & \cdots & \Psi_P(\boldsymbol{\xi}_1) \\ \vdots & \vdots & \ddots & \vdots \\ \Psi_0(\boldsymbol{\xi}_P) & \Psi_1(\boldsymbol{\xi}_P) & \cdots & \Psi_P(\boldsymbol{\xi}_P) \end{bmatrix} \begin{Bmatrix} \alpha_0 \\ \alpha_1 \\ \vdots \\ \alpha_P \end{Bmatrix} = \begin{Bmatrix} \alpha^*(\boldsymbol{\xi}_0) \\ \alpha^*(\boldsymbol{\xi}_1) \\ \vdots \\ \alpha^*(\boldsymbol{\xi}_P) \end{Bmatrix} \tag{7}$$

The spectral modes α_k of the random variable α^* are obtained by solving the linear system of equations given above. Using these, various statistics, including the mean μ_{α^*} [Eq. (5)] and the variance $\sigma^2_{\alpha^*}$ [Eq. (6)] of the solution can be obtained.

A preliminary form of point-collocation approach was first introduced by Walters [9] to approximate the polynomial chaos coefficients of the metric terms, which are required as input stochastic variables for the intrusive polynomial chaos representation of a stochastic heat transfer problem with geometric uncertainty. It should be noted that the accuracy of the point-collocation NIPC will depend on the selection of the sample points in the design space. To investigate the selection of optimum collocation points, Hosder et al. [21] applied the point-collocation NIPC to model stochastic problems with multiple uncertain input variables having uniform probability distributions and investigated different sampling techniques (random, Latin hypercube, and Hammersley). The results of the stochastic model problems showed that all three sampling methods exhibit a similar performance in terms of the accuracy and the computational efficiency of the chaos expansions. However, the convergence of the point-collocation NIPC statistics obtained with Hammersley and Latin hypercube sampling exhibit a much smoother (monotonic) convergence compared to the cases obtained with random sampling. In addition to Hammersley and Latin hypercube sampling, one can also select the collocation locations from multidimensional tensor-product quadrature points used in stochastic collocation method described by Xiu and Hesthaven [22] and Xiu [23].

The solution of linear problem given by Eq. (3) requires $P+1$ deterministic function evaluations. If more than $P+1$ samples are chosen, then the overdetermined system of equations can be solved using the least-squares approach. Hosder et al. [21] investigated this option by increasing the number of collocation points in a systematic way through the introduction of an oversampling ratio n_p defined as

$$n_p = \frac{\text{number of samples}}{P+1} \tag{8}$$

In the solution of stochastic model problems with multiple uncertain variables, they have used $n_p = 1, 2, 3$, and 4 to study the effect of the number of collocation points (samples) on the accuracy of the polynomial chaos expansions.

Their results showed that using a number of collocation points that is twice more than the minimum number required ($n_p = 2$) gives a better approximation to the statistics at each polynomial degree. This improvement can be related to the increase of the accuracy of the polynomial coefficients due to the use of more information (collocation points) in their calculation. In other words, increasing the number of collocation points help reduce the error between the polynomial chaos response surface approximation with the point-collocation NIPC and the representation with the exact chaos expansion. The results of the stochastic model problems also indicated that for problems with multiple random variables, improving the accuracy of polynomial chaos coefficients in NIPC approaches may reduce the computational expense by achieving the same accuracy level with a lower order polynomial expansion.

Figure 1 shows the computational cost associated with the point collocation and the quadrature-based NIPC (see the Appendix) methods. For the point collocation, the number of function evaluations is equal to $n_p \times (P+1)$ where $P+1$ is the number of output modes for a given polynomial degree p and number of random variables n [see Eq. (2)]. The number of function evaluations for the quadrature-based NIPC can be shown to be equal to $(p+1)^n$ (see the Appendix). For a single random variable, the number of function evaluations for each method is comparable. However, as the number of random variables increase, the computational cost of the numerical quadrature grows significantly. One may think of using an

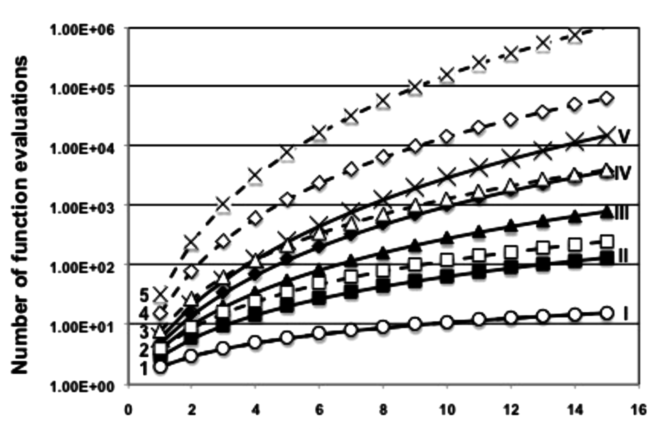

Fig. 1 Number of function evaluations for the point collocation ($n_p = 1$) and the quadrature-based NIPC as a function of polynomial chaos degree. Black-filled symbols correspond to point-collocation NIPC results with number of random variables up to 5 (Roman numerals). White-filled symbols represent the quadrature-based NIPC results with number of random of variables up to 5.

optimum number of quadrature points (polynomial degree) to reduce the cost, but for a general stochastic function or problem, considerable number of quadrature points may be required to evaluate the integration with desired accuracy as shown by Huyse et al. [18]. For both methods, the computational cost becomes formidable with the increase of the polynomial degree and the number of random variables. It should be noted that in Fig. 1 the limits of the number of function evaluations are extended to very large numbers to show the general trend. In reality, especially for large-scale stochastic computations, one can afford only a certain number of deterministic runs to the produce the output values at the selected collocation or quadrature points. This emphasizes the necessity of the implementation of innovative methods in large-scale stochastic problems to model and propagate multiple input uncertainties with desired accuracy and efficiency.

IV. Application Examples

A. Stochastic Expansion-Wave Problem

To analyze the stochastic expansion-wave problem, we consider inviscid, steady, two-dimensional, supersonic flow of a calorically perfect gas over a convex corner. Under these conditions, a centered expansion fan originates from the sharp convex corner, as shown in Fig. 2. The static pressure, which is the output quantity of interest for this problem, decreases continuously across the expansion fan and remains constant in the region downstream of the rearward Mach line. The deterministic problem involves the solution of the supersonic flowfield for a given freestream Mach number M_{ref}, specific heat ratio γ, and deflection angle θ.

To solve the deterministic problem, one may use the Prandtl-Meyer relations to calculate the Mach number at any increment of deflection angle across the expansion fan. Once the Mach number is known, the pressure drop (P/P_{ref}) can be calculated using the isentropic relations for a perfect gas. The details of the Prandtl-Meyer solution can be found in Anderson [24]. In our study, we solved the deterministic problem numerically using the CFL3D code of NASA Langley Research Center to demonstrate the application of the point-collocation NIPC method to CFD simulations. CFL3D is a three-dimensional finite volume Navier–Stokes code capable of solving steady or time-dependent aerodynamic flows ranging from subsonic to supersonic speeds [25].

We used CFL3D to solve the Euler equations, which are a subset of Navier–Stokes equations and govern the inviscid, compressible flow of a fluid. Both NIPC and Monte Carlo methods used the

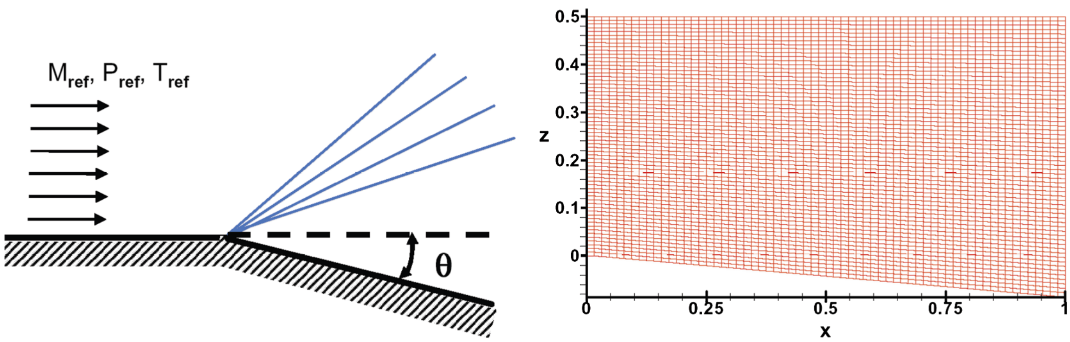

Fig. 2 Description of the supersonic, inviscid flow over a convex corner with a turn angle of θ. On the right, the mean grid (65 × 65) used in Euler computations is shown. The mean deflection angle is 5.0 deg.

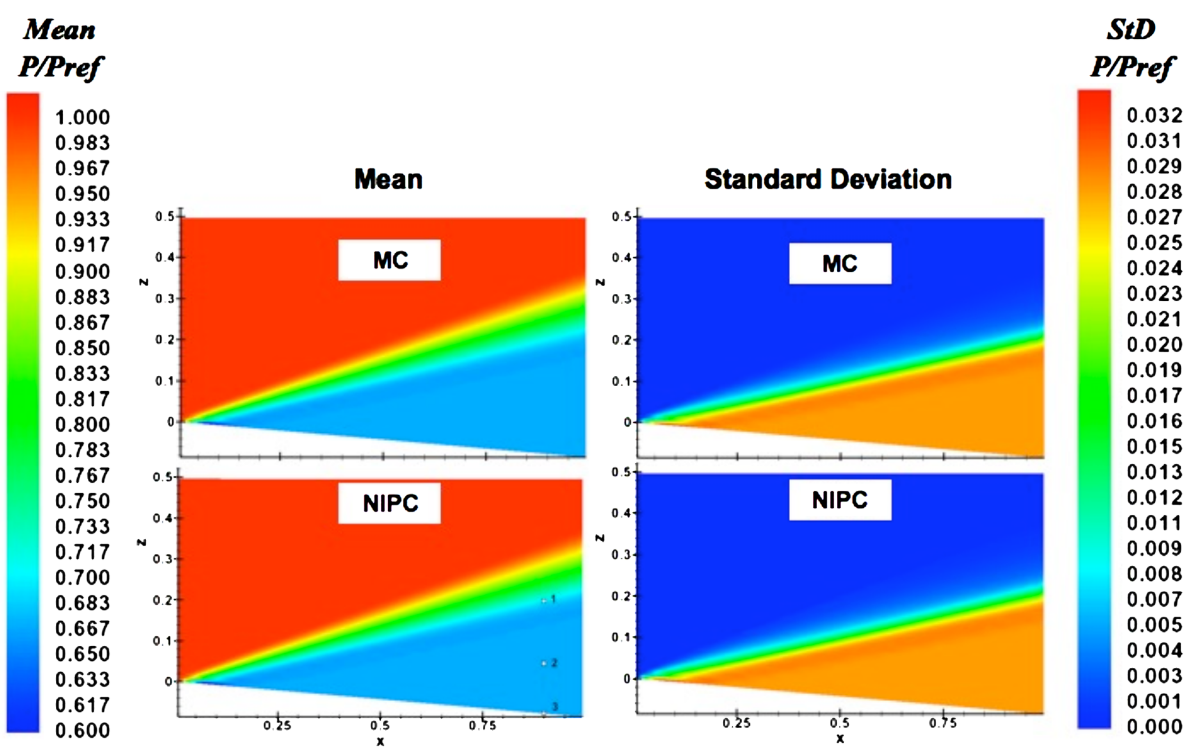

Fig. 3 Mean and standard deviation distributions of pressure (P/P_{ref}) obtained from Monte Carlo (MC) simulations and point-collocation NIPC for the supersonic expansion-wave problem. The three locations shown in the mean polynomial chaos plot designate the points where the quantitative analyses were performed.

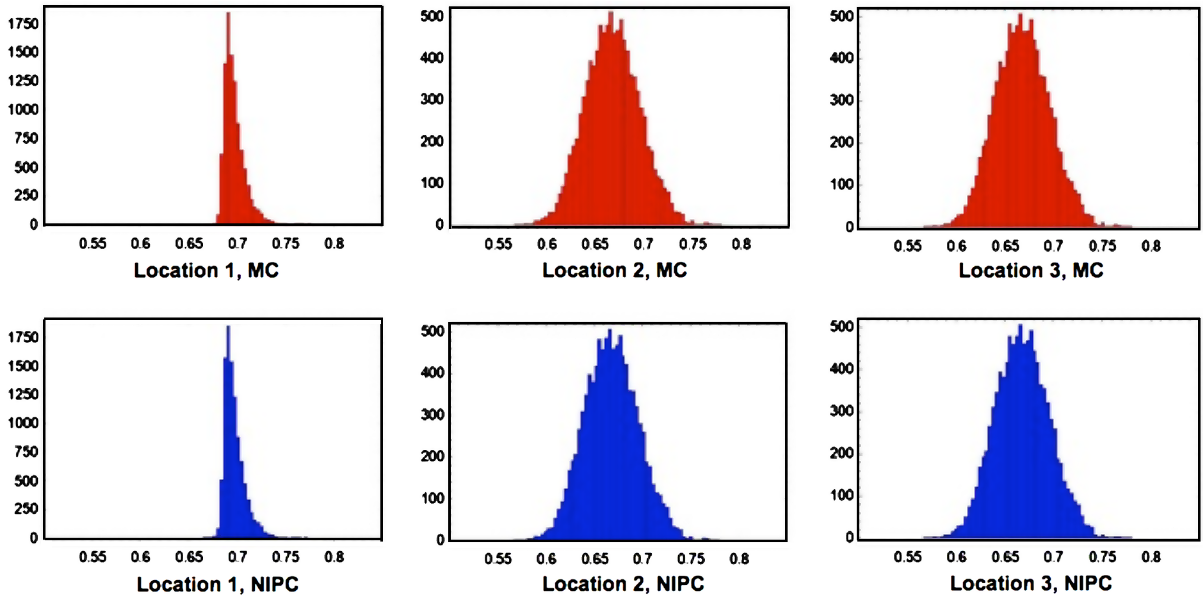

Fig. 4 Static pressure histograms obtained at three locations for the supersonic expansion-wave problem using MC and point-collocation NIPC methods.

deterministic solutions from Euler calculations in their implementation. The computations were performed on grids, which have 65 grid points in both x and z directions. Figure 2 shows the grid with the mean deflection angle, θ_{mean}. The equations were integrated in time using an implicit approximate factorization scheme to reach the steady state. A full multigrid (multigrid plus mesh sequencing) method was used for convergence acceleration. The freestream Mach number was chosen as $M_{\mathrm{ref}} = 3.0$ and the angle of attack was set to 0 deg. The inviscid fluxes on the cell faces were calculated using Roe flux difference splitting and the primitive variables on the cell faces were obtained using an upwind-bias third-order accurate scheme with the MinMod limiter.

The stochastic expansion-wave problem was formulated by introducing a geometric uncertainty through the deflection angle θ that was uncertain and described by a Gaussian distribution:

$$\theta(\xi) = \theta_{\mathrm{mean}} + \xi\sigma \tag{9}$$

The mean deflection angle was 5 deg and the coefficient of variation was 10%. Here, ξ is a normally distributed random variable with zero mean and unit variance ($\xi = N[0, 1]$). Uncertainty propagation in supersonic expansion flow has been modeled using crude Monte Carlo and the point-collocation NIPC methods. In Monte Carlo simulations, 10,000 grids were created using 10,000 samples from the $\theta(\xi)$ distribution. The Euler equations were solved on each grid using the CFL3D code. A fourth-order chaos expansion using Hermite polynomials as basis functions was chosen to model the uncertainty propagation with the NIPC method. To obtain the polynomial coefficients, five deterministic solutions were evaluated on five grids with deflection angles that correspond to $\xi_0 = 0.0$, $\xi_1 = 1.0$, $\xi_2 = -1.0$, $\xi_3 = 2.0$, and $\xi_4 = -2.0$ (e.g., the collocation locations are equally spaced in the random space). It should be noted that each deterministic solution that corresponds to a specific value of ($\theta(\xi)$) was obtained on a different grid, which has different cell center locations. Each deterministic solution was interpolated to the mean grid to calculate the Monte Carlo statistics at the cell center locations of the mean grid. Similarly, the polynomial chaos expansions for the pressure were calculated at the mean grid cell center locations using five deterministic solutions that were obtained from the interpolation of the original $\theta(\xi_i)$ $(i = 0, \ldots, 4)$ results to the mean grid.

Figure 3 gives the mean and standard deviation contours of pressure for the NIPC method and the Monte Carlo simulations. The qualitative agreement between the results of the two methods is good. Across the expansion wave, a smooth mean pressure drop is observed. The standard deviation increases smoothly across the expansion wave for all cases. To analyze the statistics of the Monte Carlo and NIPC methods quantitatively, we have picked three locations in the flowfield. All three are on the same streamwise station, but they are at different distances from the wall (Fig. 3). Location 1 ($x = 0.8984$, $z = 0.1978$) is in the expansion fan toward the rearward Mach line, location 2 ($x = 0.8984$, $z = 0.0445$) is downstream of the expansion fan, and location 3 ($x = 0.8984$, $z = -0.0772$) is a point on the wall downstream of the expansion fan. The static pressure histograms at these locations are shown in Fig. 4. At all locations, the histograms of the nonintrusive polynomial chaos

Table 1 Mean and standard deviation distributions of pressure (P/P_{ref}) obtained with MC and point-collocation NIPC methods at three selected locations for the supersonic expansion-wave problem

Location	NIPC	MC	95%-confidence interval[a]
Mean			
1	0.697085	0.697122	[0.696907, 0.697336]
2	0.668056	0.668065	[0.667515, 0.668629]
3	0.668071	0.668070	[0.667519, 0.668633]
Standard deviation			
1	0.0107491	0.0107470	[0.0104820, 0.0110103]
2	0.0280358	0.0280317	[0.0276231, 0.0284082]
3	0.0280277	0.0280260	[0.0276174, 0.0284027]

[a]The 95%-confidence intervals for the MC statistics are calculated using the bootstrap method.

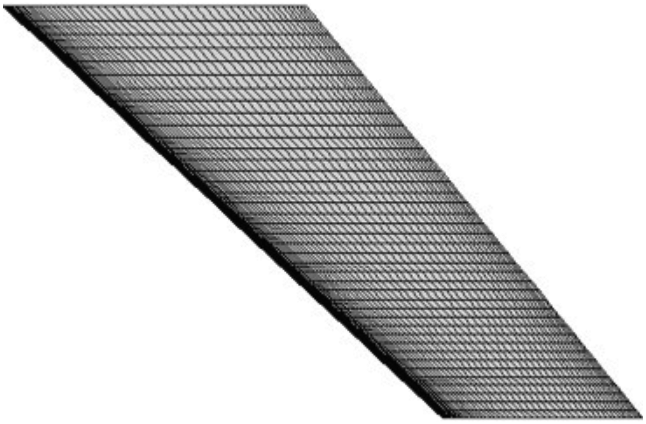

Fig. 5 AGARD 445.6 wing and the surface grid.

Table 2 Computational cost for the evaluation of Latin hypercube Monte Carlo simulations and the point-collocation NIPC for the stochastic transonic-wing problem

		NIPC[a]				
	Monte Carlo	$p = 1$	$p = 2$	$p = 3$	$p = 4$	$p = 5$
Number of CFD runs	1000	6	12	20	30	42
Wall clock time, h	46.6	0.28	0.56	0.94	1.4	1.96

[a]Here, p is the degree of polynomial chaos.

Table 3 Latin hypercube Monte Carlo statistics for C_L and C_D

	Mean	95%-confidence interval of mean[a]	Standard deviation	95%-confidence interval of standard deviation[a]
C_L	0.000169661	[−0.005324476, 0.005058219]	0.084082119	[0.081239769, 0.08641931]
C_D	0.002538528	[0.002414416, 0.002655811]	0.002164797	[0.002075901, 0.002234283]

[a]The 95%-confidence intervals for the MC statistics were calculated using the bootstrap method.

method are in good agreement with the ones obtained with the Monte Carlo simulations. The distribution at location 1 (expansion fan) is slightly skewed to the right, whereas the histograms at locations 2 and 3 follow the Gaussian distribution closely. For location 1, it can be seen that a fourth-order polynomial expansion is sufficient to model the non-Gaussian contributions observed at this region of the flow.

Table 1 gives the mean and the standard deviation of the pressure at the three stations depicted above. For each statistical quantity obtained with the Monte Carlo Simulations, a 95%-confidence interval is also presented. We use the bootstrap method to compute the confidence intervals as well as the standard error estimate of each statistical quantity. The advantage of this method is that it is not restricted to a specific distribution: e.g., a Gaussian. It is easy and efficient to implement and can be completely automated to any estimator, such as the mean or the variance. In practice, one takes 25–200 bootstrap samples to obtain a standard error estimate. In our computations, we used 500 bootstrap samples. Note that each sample consisted of 10,000 observations selected randomly from the original Monte Carlo simulations by giving equal probability $(1/10,000)$ to each observation. For all three locations, the mean and standard deviation values obtained with the NIPC method fall within the 95%-confidence intervals that were calculated for the statistics of Monte Carlo simulations. The standard deviation at location 1 is approximately 2.5 times less than the ones obtained at locations 2 and 3 for both orders of spatial accuracy. These results can also be detected visually from the histogram plots.

B. Stochastic Transonic-Wing Problem

To demonstrate the application of point-collocation NIPC to an aerospace problem with multiple uncertain input variables, a stochastic computational aerodynamics problem, which includes the numerical simulation of steady, inviscid, transonic flow over a three-dimensional wing has been selected. The wing geometry is the AGARD 445.6 aeroelastic wing [26] (Fig. 5), which has been extensively used to validate computational aeroelasticity tools especially in the determination of flutter boundary at various transonic Mach numbers. The wing has a quarter-chord sweep angle of 45 deg, a panel aspect ratio of 1.65, a taper ratio of 0.66, and a NACA 65A004 airfoil section. The current study includes the aerodynamic simulations with the rigid-wing assumption, which can be thought as a preliminary investigation before the application of the NIPC to a stochastic computational aeroelasticity problem involving the same geometry. As in the expansion-wave problem, we used CFL3D code to solve the steady Euler equations numerically. The computational grid has a C-H topology with $193 \times 65 \times 42$ points.

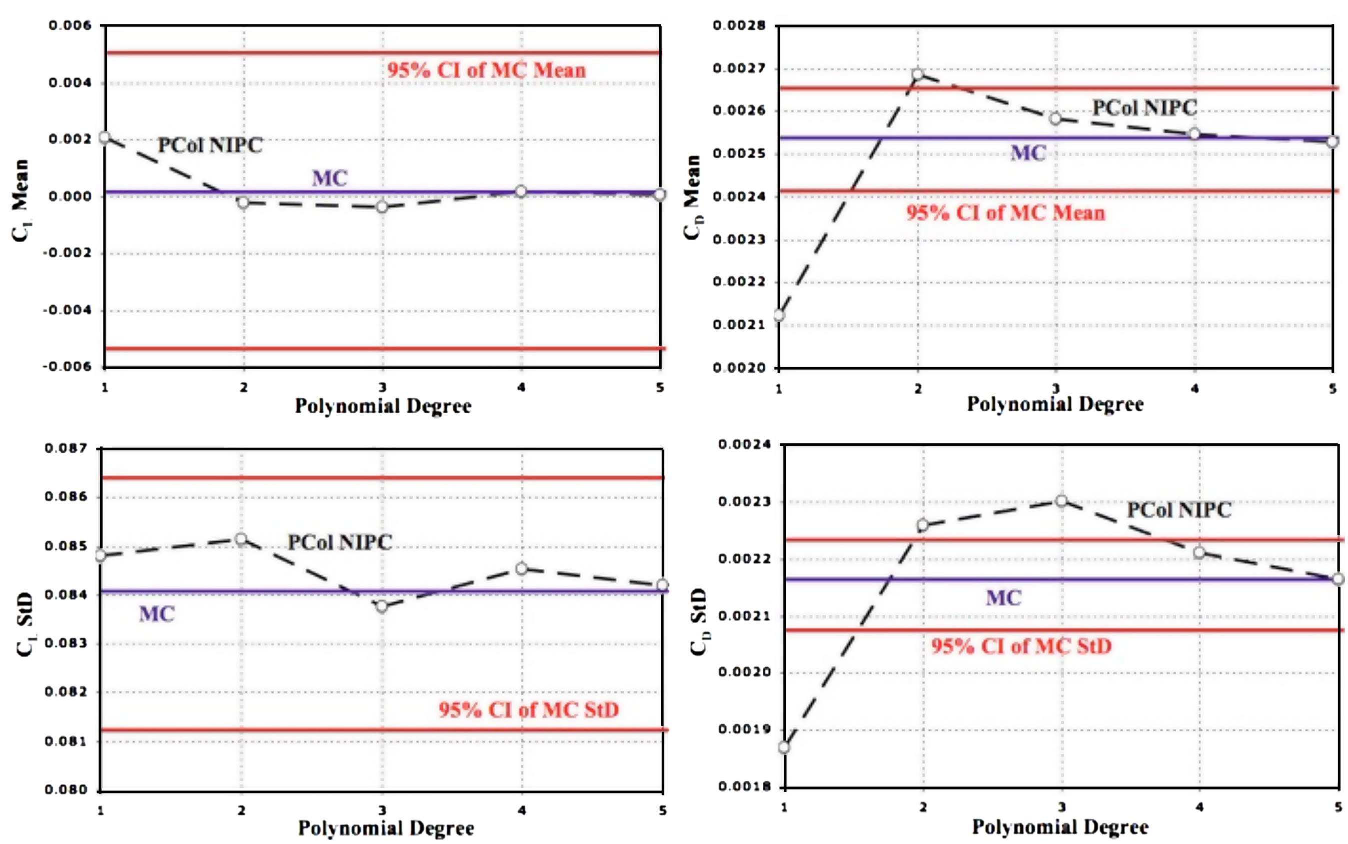

Fig. 6 Mean and standard deviation of C_L and C_D obtained with point-collocation NIPC and Latin hypercube Monte Carlo.

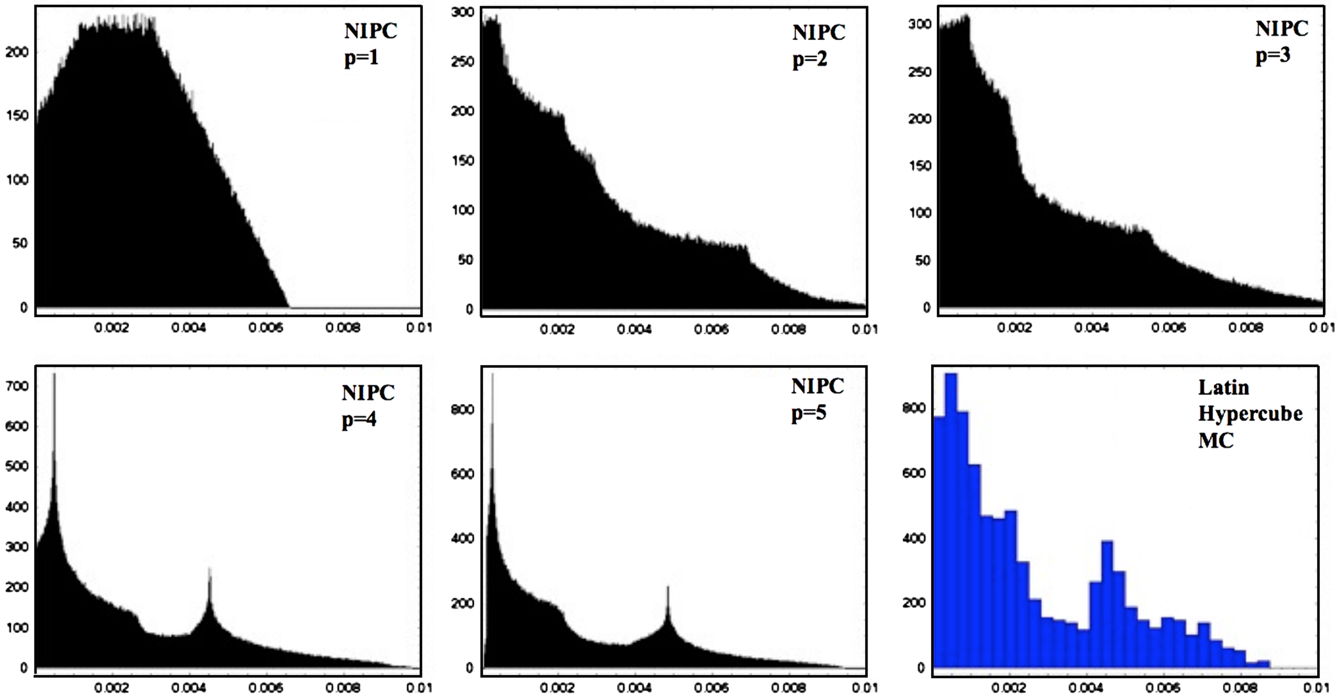

Fig. 7 Histograms of C_D obtained with the Latin hypercube Monte Carlo (MC) and NIPC.

For the stochastic aerodynamics problem, the freestream Mach number M_{ref} and the angle of attack α are treated as uncertain variables. The Mach number is modeled as a uniform random variable between $M_\infty(\xi_1) = 0.8$ and 1.1, and the angle of attack is defined as a uniform random variable between $\alpha(\xi_2) = -2.0$ and 2.0 deg. Note that each component of the random variable vector $\boldsymbol{\xi} = \{\xi_1, \xi_2\}$ is a uniform random variable defined in the interval $[-1, 1]$. Therefore, in our NIPC calculations, we have used multidimensional Legendre polynomials that are orthogonal in the interval $[-1, 1]$ for each random dimension. Stochastic solutions to

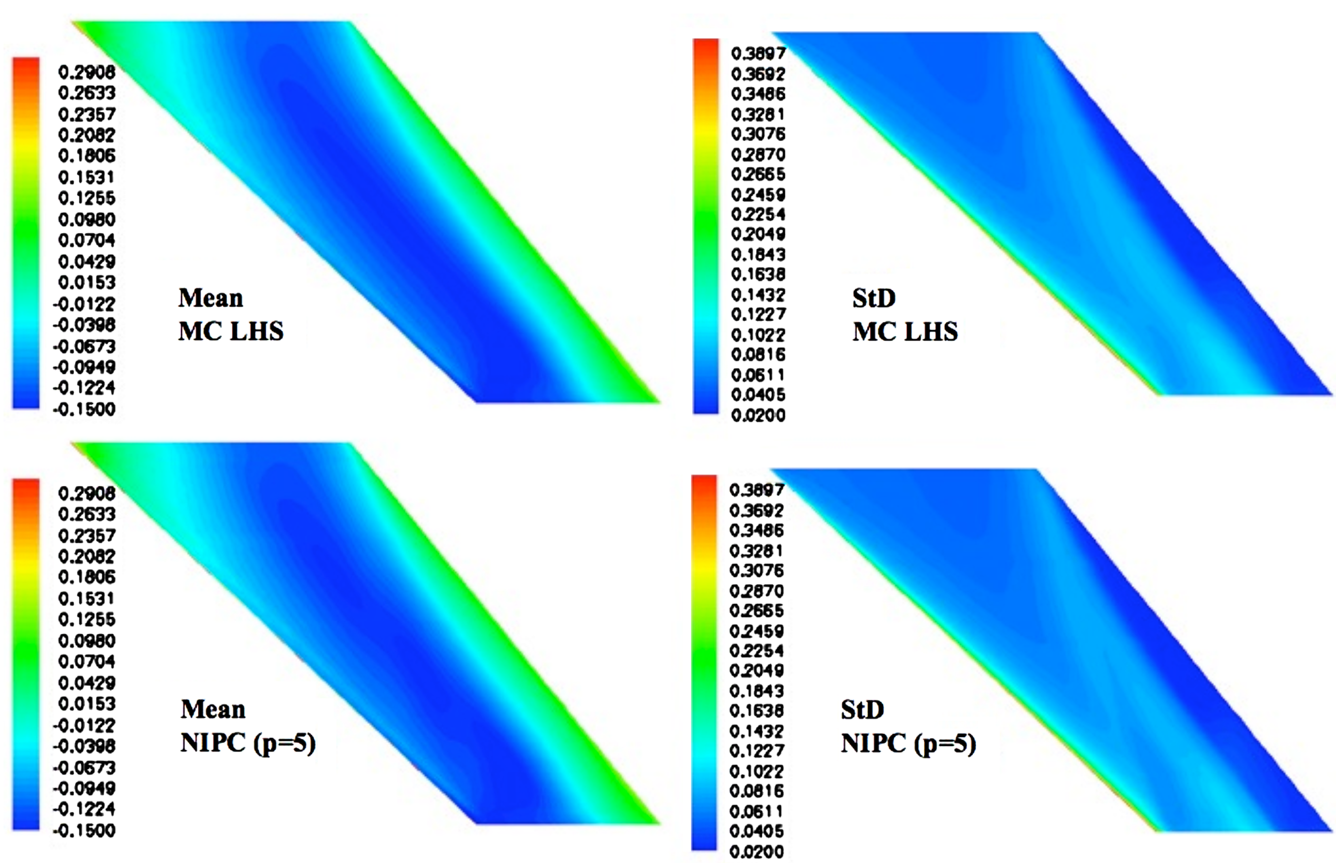

Fig. 8 Mean and standard deviation of pressure coefficient C_p on the upper surface of the AGARD 445.6 wing. The point-collocation NIPC results are obtained with fifth-degree chaos expansions.

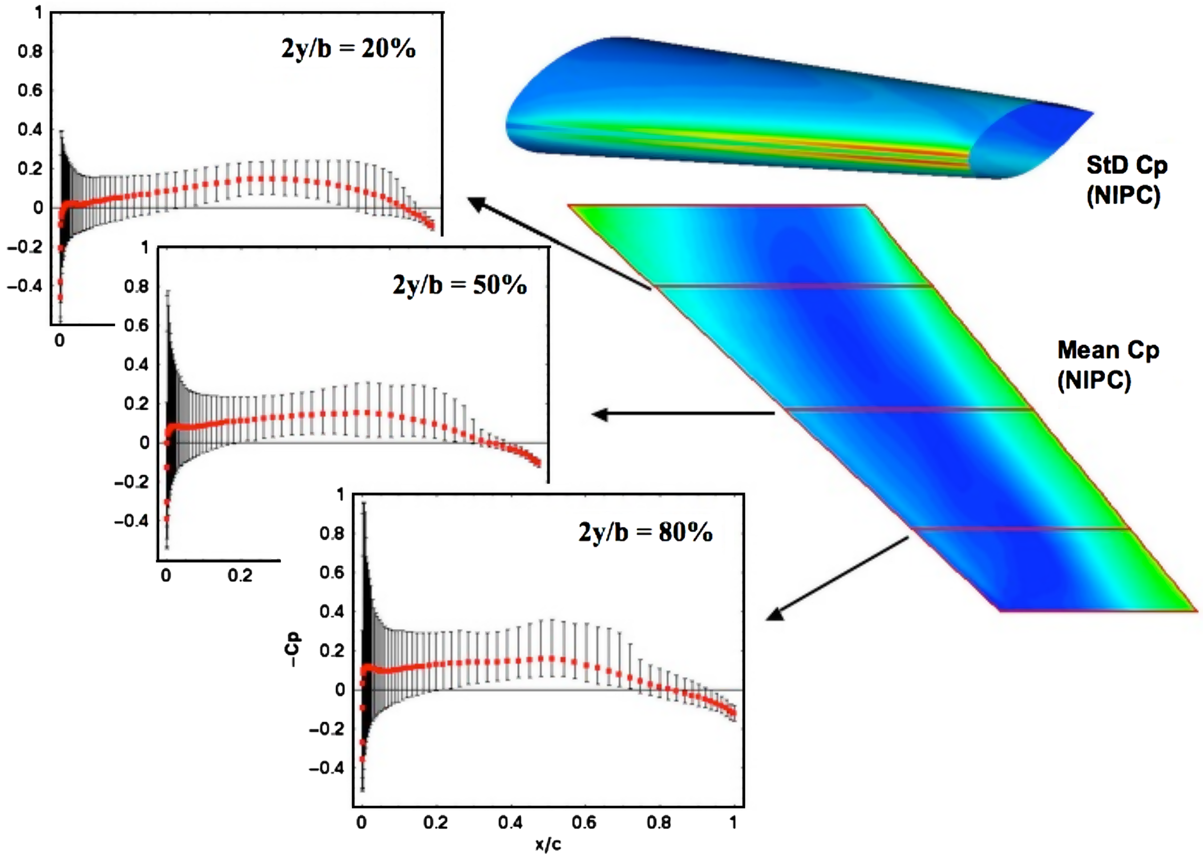

Fig. 9 Uncertainty bars for the upper-surface C_p distributions of the AGARD 445.6 wing at three spanwise stations. The uncertainty bars include C_p values within 95%-confidence intervals obtained with the point-collocation NIPC method.

the problem were obtained with two approaches: Latin hypercube Monte Carlo with 1000 samples and point-collocation NIPC. Based on the observations from the stochastic model problems studied [21], Hammersley sampling with $n_p = 2$ has been used for the selection of collocation points for the NIPC approach. The chaos expansions were obtained up to a polynomial degree of five. Table 2 gives the computational cost associated with each stochastic approach. As can be seen from this table, on the same computer (SGI Origin 3800 with 64 processors used), it took 46.6 h to finish the Monte Carlo simulations, whereas the computational time was approximately 2 h for the point-collocation NIPC with a polynomial degree of five.

Table 3 gives the statistics and the 95%-confidence intervals of the lift C_L and drag C_D coefficient obtained with the Latin hypercube Monte Carlo simulations. In Fig. 6, the convergence of C_L and C_D statistics obtained with the point-collocation NIPC is presented. For all polynomial degrees, the NIPC approximations to the mean and the standard deviation of the lift coefficient stays within the 95%-confidence interval of the Monte Carlo statistics. The mean of the drag coefficient falls within the confidence interval at a polynomial degree of three, whereas the standard deviation enters the interval with a polynomial degree of four.

The histogram of the drag coefficient obtained with the NIPC approach gets very similar to the histogram shape of the Monte Carlo simulations at a polynomial degree of five (Fig. 7). The mean and the standard deviation distributions of the pressure coefficient C_p on the wing upper surface are given in Fig. 8. The Monte Carlo and the NIPC statistics are in a good qualitative agreement in most regions of the wing. Overall, this computational example shows that a fifth-degree point-collocation NIPC expansion obtained with Hammersley sampling and $n_p = 2$ is capable of estimating the statistics at an accuracy level of 1000 Latin hypercube Monte Carlo simulations with a significantly lower computational cost.

Using the NIPC expansions, one can also efficiently obtain the complete probability distribution (histogram) of any flow quantity at any point in the flowfield. This information is especially important for the surface pressure distributions, which are often used for comparison with the experimental data in CFD validation studies. With the complete probability distribution information, it is possible to calculate the confidence intervals for the CFD results, which may be uncertain due to the variations in various input parameters such as the freestream Mach number or the angle of attack studied in the present stochastic transonic-wing study. Figure 9 shows the uncertainty bars for the upper-surface C_p distributions on the AGARD 445.6 wing at three spanwise stations. These uncertainty bars include the C_p values within 95%-confidence intervals obtained with the point-collocation NIPC method. As can also be seen from the contour plot of the standard deviation, the largest uncertainty in pressure is located in the leading-edge region toward the tip of the wing.

V. Conclusions

In this paper, a point-collocation NIPC method has been introduced as a computationally efficient uncertainty modeling and propagation method that can be applied to stochastic CFD simulations. The method is nonintrusive, in the sense that no modification to the deterministic code is required, which is a significant benefit for uncertainty quantification in complex fluid dynamics simulations. The application of point-collocation NIPC to stochastic CFD has been demonstrated with two examples: 1) a stochastic expansion wave problem with an uncertain deflection angle (geometric uncertainty) and 2) a stochastic transonic-wing case with uncertain freestream Mach number and angle of attack. For both cases, various statistics were computed with both the NIPC method and Monte Carlo technique. Confidence intervals for Monte Carlo statistics were calculated using the bootstrap method. For the expansion-wave problem, a fourth-degree polynomial chaos expansion, which required five deterministic evaluations, was sufficient to predict the statistics within the confidence interval of 10,000 crude Monte Carlo simulations. In the transonic-wing case, for various output quantities of interest, it has been shown that a fifth-degree point-collocation NIPC expansion obtained with Hammersley sampling was capable of estimating the statistics at an accuracy level of 1000 Latin hypercube Monte Carlo simulations with a significantly lower computational cost.

Overall, the examples demonstrated that the point-collocation NIPC has a promising potential as an effective and computationally efficient uncertainty propagation method in stochastic CFD problems. The investigation and implementation of techniques for the determination of optimum polynomial degree and the selection of optimum collocation points will further improve the accuracy and the computational efficiency of the method.

Appendix

To find the polynomial coefficients $\alpha_k = \alpha_k(\mathbf{x})$, $(k = 0, 1, \ldots, P)$ in Eq. (1) using sampling-based and quadrature methods, the equation is projected onto kth basis:

$$\langle \alpha^*(\mathbf{x}, \boldsymbol{\xi}), \Psi_k(\boldsymbol{\xi})\rangle = \left\langle \sum_{j=0}^{P} \alpha_j(\mathbf{x})\Psi_j(\boldsymbol{\xi}), \Psi_k(\boldsymbol{\xi}) \right\rangle \tag{A1}$$

Using the orthogonality of the basis functions,

$$\langle \alpha^*(x, \boldsymbol{\xi}), \Psi_k(\boldsymbol{\xi})\rangle = \alpha_k \langle \Psi_k^2(\boldsymbol{\xi})\rangle \tag{A2}$$

we can obtain

$$\alpha_k(\mathbf{x}) = \frac{\langle \alpha^*(\mathbf{x}, \boldsymbol{\xi}), \Psi_k(\boldsymbol{\xi})\rangle}{\langle \Psi_k^2(\boldsymbol{\xi})\rangle} = \frac{1}{\langle \Psi_k^2(\boldsymbol{\xi})\rangle} \int_R \alpha^*(\mathbf{x}, \boldsymbol{\xi})\Psi_k(\boldsymbol{\xi}) p(\boldsymbol{\xi})\, \mathrm{d}\boldsymbol{\xi} \tag{A3}$$

In sampling-based methods, the main strategy is to compute the product $\alpha^*(x, \boldsymbol{\xi})\Psi_k(\boldsymbol{\xi})$ for a number of samples (ξ_i, $i = 1, \ldots, N_{\text{samples}}$) and perform averaging to determine the estimate of the inner product $\langle \alpha^*(x, \boldsymbol{\xi}), \Psi_k(\boldsymbol{\xi})\rangle$. Quadrature methods calculate the same term, which is an integral over the support of the weight function $p_N(\boldsymbol{\xi})$, using numerical quadrature. Once this term is evaluated, both methods (sampling-based and quadrature) use Eq. (A3) to estimate the projected polynomial coefficients for each mode.

Similar to Monte Carlo methods, the accuracy of sampling approach will depend on the number of samples used to approximate the expectation. To evaluate the integral in the numerator of Eq. (A3) for one-dimensional problems with the quadrature-based approach, the straightforward procedure will be to use Gaussian quadrature points, which are zeros of orthogonal polynomials that are optimal for the given input uncertainty distribution (i.e., Gauss–Hermite, Gauss–Legendre, and Gauss–Laguerre points for normal, uniform, and exponential distributions, respectively). The extension of this approach to multidimensional problems can be achieved via tensor product of one-dimensional quadrature formulas. For a one-dimensional problem, if the polynomial degree for the chaos expansion is chosen as p, then the minimum number of quadrature points required for the exact evaluation of the integral will be $p + 1$, since a Gauss quadrature formula of p points will evaluate a polynomial of $2p - 1$ degree or less exactly and the polynomial degree of the product of the function approximation and the basis in the integrand of the numerator term in Eq. (A3) will be $2p$ for the evaluation of the highest-degree coefficient. For stochastic problems with small number of input uncertain variables, this approach will be efficient, however, for multidimensional problems the computational cost will be significant due to its exponential growth with the number of random dimensions. The required number of deterministic function evaluations will be $(p + 1)^n$ for a stochastic problem with n random variables having the same degree of polynomial expansion (p) in each dimension. An alternative approach for more efficient evaluation of the multidimensional integrals will be to use sparse tensor-product spaces instead of full tensor product of Gauss quadrature points to cover the multidimensional random space (see [19,22,23] for details).

References

[1] Walters, R. W., and Huyse, L., "Uncertainty Analysis for Fluid Mechanics with Applications," NASA Langley Research Center, CR-2002-211449, Hampton, VA, 2002.

[2] Ghanem, R., and Spanos, P. D., "Polynomial Chaos in Stochastic Finite Elements," *Journal of Applied Mechanics*, Vol. 57, March 1990, pp. 197–202.
doi:10.1115/1.2888303

[3] Ghanem, R. G., and Spanos, P. D., *Stochastic Finite Elements: A Spectral Approach*, Springer–Verlag, New York, 1991.

[4] Ghanem, R., "Stochastic Finite Elements with Multiple Random Non-Gaussian Properties," *Journal of Engineering Mechanics*, Vol. 125, Jan. 1999, pp. 26–40.
doi:10.1061/(ASCE)0733-9399(1999)125:1(26)

[5] Ghanem, R. G., "Ingredients for a General Purpose Stochastic Finite Element Formulation," *Computer Methods in Applied Mechanics and Engineering*, Vol. 168, 1999, pp. 19–34.
doi:10.1016/S0045-7825(98)00106-6

[6] Mathelin, L., Hussaini, M., Zang, T., and Bataille, F., "Uncertainty Propagation for Turbulent, Compressible Nozzle Flow Using Stochastic Methods," *AIAA Journal*, Vol. 42, No. 8, Aug. 2004, pp. 1669–1676.
doi:10.2514/1.5674

[7] Xiu, D., and Karniadakis, G. E., "Modeling Uncertainty in Flow Simulations via Generalized Polynomial Chaos," *Journal of Computational Physics*, Vol. 187, No. 1, May 2003, pp. 137–167.
doi:10.1016/S0021-9991(03)00092-5

[8] Wiener, N., "The Homogeneous Chaos," *American Journal of Mathematics*, Vol. 60, No. 4, 1938, pp. 897–936.
doi:10.2307/2371268

[9] Walters, R., "Towards Stochastic Fluid Mechanics via Polynomial Chaos," 41st AIAA Aerospace Sciences Meeting and Exhibit, Reno, NV, AIAA Paper 2003-0413, Jan. 2003.

[10] Perez, R., and Walters, R., "An Implicit Compact Polynomial Chaos Formulation for the Euler Equations," 43rd AIAA Aerospace Sciences Meeting and Exhibit, Reno, NV, AIAA Paper 2005-1406, Jan. 2005.

[11] Najm, H. N., "Uncertainty Quantification and Polynomial Chaos Techniques in Computational Fluid Dynamics," *Annual Review of Fluid Mechanics*, Vol. 41, 2009, pp. 35–52.
doi:10.1146/annurev.fluid.010908.165248

[12] Debusschere, B. J., Najm, H. N., Pebay, P. P., Knio, O. M., Ghanem, R. G., and Maitre, O. P. L., "Numerical Challenges in the Use of Polynomial Chaos Representations for Stochastic Processes," *SIAM Journal on Scientific Computing*, Vol. 26, No. 2, 2004, pp. 698–719.
doi:10.1137/S1064827503427741

[13] Reagan, M., Najm, H. N., Ghanem, R. G., and Knio, O. M., "Uncertainty Quantification in Reacting Flow Simulations through Non-Intrusive Spectral Projection," *Combustion and Flame*, Vol. 132, 2003, pp. 545–555.
doi:10.1016/S0010-2180(02)00503-5

[14] Isukapalli, S. S., "Uncertainty Analysis of Transport-Transformation Models," Ph.D. Dissertation," Rutgers, The State University of New Jersey, New Brunswick, NJ, 1999.

[15] Mathelin, L., Hussaini, M. Y., and T. Z., "Stochastic Approaches to Uncertainty Quantification in CFD Simulations," *Numerical Algorithms*, Vol. 38, No. 1, March 2005, pp. 209–236.
doi:10.1007/s11075-004-2866-z

[16] Loeven, G. J. A., Witteveen, J. A. S., and Bijl, H., "Probabilistic Collocation: An Efficient Non-Intrusive Approach for Arbitrarily Distributed Parametric Uncertainties," 45th AIAA Aerospace Sciences Meeting and Exhibit, Reno, NV, AIAA Paper 2007-317, Jan. 2007.

[17] Wiener, N., and Wintner, A., "The Discrete Chaos," *American Journal of Mathematics*, Vol. 65, No. 2, 1943, pp. 279–298.
doi:10.2307/2371816

[18] Huyse, L., Bonivtch, A. R., Pleming, J. B., Riha, D. S., Waldhart, C., and Thacker, B. H., "Verification of Stochastic Solutions Using Polynomial Chaos Expansions," 47th AIAA/ASME/ASCE/AHS/ASC Structures, Structural Dynamics, and Materials Conference, Newport, RI, AIAA Paper 2006-1994, May 2006.

[19] Eldred, M. S., Webster, C. G., and Constantine, P. G., "Evaluation of Non-Intrusive Approaches for Wiener-Askey Generalized Polynomial Chaos," 10th AIAA Non-Deterministic Approaches Forum, Schaumburg, IL, AIAA Paper 2008-1892, April 2008.

[20] Witteveen, J. A. S., and Bijl, H., "Modeling Arbitrary Uncertainties Using Gram–Schmidt Polynomial Chaos," 44th AIAA Aerospace Sciences Meeting and Exhibit, Reno, NV, AIAA Paper 2006-0896, Jan. 2006.

[21] Hosder, S., Walters, R., and Balch, M., "Efficient Sampling for Non-Intrusive Polynomial Chaos Applications with Multiple Uncertain Input Variables," 9th AIAA Non-Deterministic Approaches Conference, Honolulu, AIAA Paper 2007-1939, April 2007.

[22] Xiu, D., and Hesthaven, J., "Higher-Order Collocation Methods for Differential Equations with Random Inputs," *SIAM Journal on Scientific Computing*, Vol. 27, No. 3, 2005, pp. 1118–1139. doi:10.1137/040615201

[23] Xiu, D., "Efficient Collocational Approach for Parametric Uncertainty Analysis," *Communications in Computational Physics*, Vol. 2, No. 2, April 2007, pp. 293–309.

[24] Anderson, J. D., *Modern Compressible Flow with Historical Perspective*, 3rd ed., McGraw–Hill, New York, 2003.

[25] Krist, S. L., Biedron, R. T., and Rumsey, C. L., "CFL3D User's Manual (Version 5.0)," NASA Langley Research Center, TM-1998-208444, Hampton, VA, 1998.

[26] "AGARD Standard Aeroelastic Configurations for Dynamic Response I—Wing 445.6," NASA TM-100492, 1987.

X. Zhong
Associate Editor